Materials and Design 39 (2012) 220–225

Contents lists available at SciVerse ScienceDirect

Materials and Design

journal homepage: www.elsevier.com/locate/matdes

Effect of strain-modified particles on the formation of fined grains and the properties of AA7050 alloy

Yujing Lang [a], Hua Cui [b], Yuanhua Cai [a], Jishan Zhang [a,*]

[a] State Key Laboratory for Advanced Metals and Materials, University of Science and Technology Beijing, Xueyuan Road 30, Haidian District, Beijing 100083, PR China
[b] School of Materials Science and Engineering, University of Science and Technology Beijing, Xueyuan Road 30, Haidian District, Beijing 100083, PR China

ARTICLE INFO

Article history:
Received 5 December 2011
Accepted 4 February 2012
Available online 13 February 2012

Keywords:
A. Non-ferrous metals and alloys
E. Mechanical
F. Microstructure

ABSTRACT

With a new two-pass deformation, a fine-grained AA7050 alloy was obtained owing to small particles which can affect the grain refinement. The banded structures were produced in the elongated grain interiors after the 1st-pass deformation at 300 °C. And deformation bands containing dislocation arrays and small spherical particles were obtained. A few new fined grains appeared along the elongated grain boundaries. After the 2nd-pass deformation at 430 °C, isolated chains of new fine grains were developed in the elongated grain interiors. The boundary glide and the increase of grain boundary misorientation due to cumulative strain could refine the elongated grains. The pinning effect of the particles accelerated the formation of deformation bands. The increase of deformation temperature promoted the rapid evolution of grain refinement during the deformation. The strength of the fine-grained AA7050 alloy was enhanced while the ductility was decreased.

1. Introduction

The specific grain structure of the aerospace aluminum alloys can be obtained by controlling the composition and the process and the balance among different properties is desired to meet the specific requirements for future airframes [1]. Especially, the 7xxx aluminum alloys with high strength to weight ratio are primarily concerned in the aerospace industry. The fine-grained aluminum alloys have higher strength and lower ductility than coarse grained alloys [2,3]. And the recrystallized grains can induce many defects, such as continuous grain boundary precipitate (GBP) [4], grain boundary precipitate-free zone (PFZ) [5] and intergranular fracture [6]. Therefore, controlling the recrystallization and grain sizes of aluminum alloys during the plastic deformation is crucial for the properties and applications [7,8]. Different methods have been performed to obtain fined and unrecrystallized grains in 7xxx aluminum alloys [7,9–15]. For example, (Zr, Sc)-alloying can inhibit the recrystallization and enhance stress corrosion cracking resistance [9] in Al–Zn–Mg–Cu alloys, and the severe plastic deformation (SPD) has been used to modify the grain structures, the fraction of high angle grain boundaries (HAGBs) and the mechanical behavior [10].

Recently, the SPD [8,10–13] and cryorolling [14,15] processes have been used extensively to produce fine-grained structures and resolve the limitation of conventional processing. It is well proved that either dislocation glide or diffusivity-controlled grain boundary glide might be dominated during SPD processing of aluminum alloys at high temperature (>300 °C) [11]. And the deformation at cryogenic temperature (e.g., cryorolling) can suppress the dynamic recovery and induce high density dislocations [16,17]. But the requirement of large plastic strain and cryogenic temperature for grain refinement, and the difficulties in producing long length metals or alloys will limit the use of the SPD and cryorolling. Moreover, the fine-grained structures in aluminum alloys are very difficult to get by conventional rolling process because of the high stacking fault energy of aluminum alloys. However, for grain refinement, the particles play an important role during conventional rolling [18–20] and SPD [12,21], for example, small particles can inhibit the recrystallization while large particles can stimulate nucleation (PSN) for recrystallization [18–20]. In this work, a fine-grained structure in AA7050 alloy was obtained by a simple deformation processing, which was due to small and dispersed particles. The effects of the small particles on the deformation structure and grain refinement were discussed.

2. Experimental details

The AA7050 commercial hot-rolled plate with chemical compositions (wt.%): Zn: 5.7–6.7, Mg: 1.9–2.6, Cu: 2.0–2.6, Zr: 0.08–0.15, Si: <0.12, Fe: <0.15, Mn: <0.10, Cr: <0.04, Ti: <0.06, was solution treated at 480 °C × 16 h + 483 °C × 8 h and then rapidly quenched into

* Corresponding author. Tel.: +86 10 62334717.
E-mail address: zhangjs@skl.ustb.edu.cn (J.S. Zhang).

0261-3069/$ - see front matter © 2012 Elsevier Ltd. All rights reserved.
doi:10.1016/j.matdes.2012.02.005

room temperature water (SQ). The samples with $\Phi 10 \times 15$ mm machined from the SQ-treated alloy were deformed on the Gleeble-1500 thermo-mechanical simulator by two routes: Route A [22] and Route B (two-pass deformation process) in which the cylinder samples were heated with the rate of 2 °C/s to 300 °C for 120 s, and deformed with a strain rate of 10 s^{-1} to strain of 0.8 (1st-pass deformation), and followed by heating with the same heating rate to 430 °C for 10 s and deforming with a strain rate of 0.1 s^{-1} to a total strain of 1.4 with subsequent room-temperature water-quenching (2nd-pass deformation).

Microstructures were observed using optical microscopy (OM), transmission electron microscope (TEM). Electron back-scattered diffraction (EBSD) made on a LEO1450 SEM was used to analyze the sizes/orientations of the grains or sub-grains and the misorientation angles across grain boundaries. The thin foils for TEM and EBSD observation were prepared by twin-jet electro-polishing with the solution of 70% methanol and 30% nitric acid at −20 °C. XRD measurements were taken on a Rigaku X-ray diffractometer (D/MAX-RB) equipped with a Cu target ($\lambda = 0.15406$ nm) operating at 40 kV. For tensile testing [23], the specimens were cut into non-standard dog-bone-shaped specimens with a gauge length of 15 mm, a width of 3 mm and a thickness of 1.5 mm. The tensile tests were performed at room temperature with a strain rate of 10^{-3} s^{-1} along the rolling direction (RD). Three specimens were used for each condition to obtain consistent stress–strain curves. The use of miniature specimens has been previously investigated, and the specimen size and geometry only affect the postnecking elongation [24,25].

3. Results and discussion

3.1. Deformation behavior

The stress–strain curve in Fig. 1 for two-pass deformation at different strains of 10 s^{-1} (300 °C) and 0.1 s^{-1} (430 °C) shows a sharp peak just after yielding and the work softening takes place at $\varepsilon \approx 0.1$ (300 °C) that followed by a steady-state deformation during the 1st-pass deformation. The flow softening is commonly induced by dynamic recovery and recrystallization or coarsening of the precipitates [26]. But increasing the temperature to 430 °C during the 2nd-pass deformation promotes strain hardening (from 0.8 to 1.4 strain) although the flow stress decreases rapidly, which shows a different deformation behavior from that of conventional rolling.

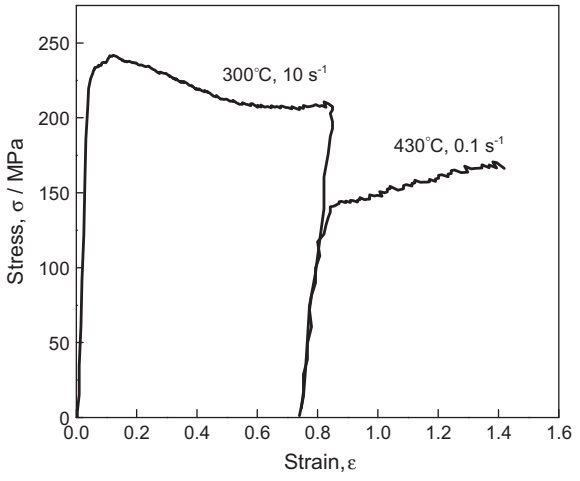

Fig. 1. Stress–strain curve obtained during two-pass deformation process for AA7050 alloy.

3.2. Grain refinement

Fig. 2a shows the solution treated alloy is characterized by larger grains and a few equiaxed grains that formed by the static recrystallization in the original grain boundaries during the solution treatment. After the 1st-pass deformation at 300 °C, the banded structures are generated in the elongated grains interior, and then the deformation bands develop as shown in Fig. 2b. Colonies of new fine grains with HAGBs ($\theta > 15°$) are only evolved along original grain boundaries at strain 0.8 (Fig. 2d). The elongated grain boundaries are the HAGBs. The low angle grain boundaries (LAGBs) ($2° < \theta < 15°$) have low misorientations and cross the elongated grain interiors. Grain orientations parallel to the *Z*-axis were marked by different colors according to the inverse pole figure (IPF) shown in the inset of Fig. 2f. The orientation variation is small in a grain, but the orientation variation is large in adjacent grains (Fig. 2f). After the 2nd-pass deformation at 430 °C, lots of new fined grains appear in the deformation band zones with jagged and fluctuant grain boundary (Fig. 2c) as well as dislocation boundaries with high and low misorientations at cumulative strain 1.4. The elongated grains are divided into new fined grains. It is difficult to distinguish the original grain boundaries with HAGBs forming from the grain subdivision (Fig. 2e). The misorientation angles among the boundaries of these banded structures increase rapidly with strain increase, and steadily transform into HAGBs, which induces fine-grained structures with d_{ave} (average grain size) = 8 μm in a whole area at strain 1.4 (Fig. 2g). Fig. 3 shows a bimodal distribution of the grain size in the 2nd-pass deformed alloy and it can be observed more clearly in Fig. 2e. It is approved that grain refinement is more obvious with more increasing strain [13].

3.3. Particle effect

TEM micrographs in Fig. 4 shows the evolution of particles and sub-grains during the deformation. After the 1st-pass deformation at 300 °C, a large number of small spherical particles (about 25 nm in mean diameter) are wrapped by the high density of dislocation cells (Fig. 4a). Fig. 4b shows the elongated cell substructures are separated by the deformation bands and a high density of dislocations pile up at the deformation bands (inset Fig. 4b). Fig. 5 shows strong $MgZn_2$ peaks in the 1st-pass deformed alloy, which confirms that the particles are largely obtained during the deformation at 300 °C, while minor $MgZn_2$ peaks are detected in the 2nd-pass deformed alloy. Because some particles are dissolved into the Al matrix that promotes other particles to grow and coarsen, such as spheroid-like and rod-like the particles in Fig. 4c, so that the particles' density is decreased after the 2nd-pass deformation at 430 °C. These particles can pin the intragranular dislocations and prevent the grain boundaries migration, inducing the formation of the sub-grains. The Fig. 4d shows the distribution of the sub-grains in the 2nd-pass deformed AA7050 alloy. It is clear that, in this alloy, banded arrays are composed of sub-grain boundaries with low misorientations, and the MSBs are composed of sub-grain cells with low orientations. The sub-grains in the MSBs are finer than that in banded grain interiors. The fine-grained structures are developed mainly by formation of microshears (MSBs), and the MSBs increase the number of fined grains and boundary misorientation [13,27]. The deformation bands transform into the MSBs during the deformation, the details can be seen in Ref. [28].

Experimental results show that two-pass deformation can refine grains obviously and the distribution and the size of fined grains at strain of 1.4 by the two-pass deformation are equivalent to that of fined grains at strain of 2.8 by multi-directional forging (MDP) [13]. It is indicated that the particles can promote the role of the strain in the evolution of fine-grained structure during the deformation. There are three reasons for the promotion: first, the